Punching shear tests on RC flat slabs strengthened with an UHPFRC layer

Aurélio Sine[1], Mário Pimentel[2,*], Sandra Nunes[3]

1. PhD candidate, CONSTRUCT-LABEST, Faculty of Engineering, University of Porto, Portugal
2. Assistant Professor, CONSTRUCT-LABEST, Faculty of Engineering, University of Porto, Portugal
3. Assistant Professor, CONSTRUCT-LABEST, Faculty of Engineering, University of Porto, Portugal

[*]Corresponding author email: mjsp@fe.up.pt

Abstract

It has been shown that strengthening of existing reinforced concrete flat slabs with a thin (30 to 50 mm) ultra-high performance fibre-reinforced cementitious composite (UHPFRC) layer provides a substantial increase in both the flexural and punching shear capacity, most notably when the UHPFRC layer is reinforced with ordinary steel bars. In this work, the scarce existing experimental evidence concerning the punching shear behaviour of this type of slabs is extended with the results of six new experimental tests. The studied variables are reinforcement ratio in the original slab and in the strengthening layer, the shape of the loading area and the load eccentricity. The results of one unstrengthened specimen and of one specimen strengthened with an ordinary reinforced concrete layer are also given for reference. The observed failure modes are discussed and failure loads are compared with the estimates obtained with a failure criterion based on the critical shear crack theory.

Keywords: *Ultra-high performance fibre reinforced cementitious composites (UHPFRC); punching shear; flat slabs; strengthening; failure criterion.*

1. Introduction

Reinforced concrete (RC) flat slabs are largely used in multi storey buildings due to the ease of construction, aesthetic convenience and adaptability to equipment installation. The design of RC flat slabs is often governed by the punching shear safety check. As punching shear is associated to a brittle failure mode, design or construction errors can lead to catastrophic scenarios (Lew et al. 1982; Gardner, Huh, and Chung 2002; Wood 2003; King and Delatte 2004).

Traditional techniques for strengthening existing RC flat slabs can be divided in four groups according to the type of intervention, namely: enlargement of the supported area; strengthening of the flexural reinforcement; post-installed shear reinforcement; and post-tensioning (Koppitz, Kenel, and Keller 2013; Lapi, Ramos, and Orlando 2019). The second group comprises application of fibre reinforced polymers or of an additional layer of reinforcement over the top surface of the slab. This reinforcement is embedded in a cementitious material adhering to the roughened substrate. The most common solution for this strengthening overlay consists in the adoption of normal strength concrete (NSC) (Lapi et al. 2018b; Fernandes 2019).

The outstanding durability and mechanical properties of UHPFRC make it an eligible cementitious material for sustainable and enhanced protection and/or strengthening of RC existing structures. The addition of thin layers (h_U=30-50 mm) of UHPFRC has been proven a particularly efficient flexural strengthening method, particularly when this layer is reinforced with ordinary steel bars (Habel, Denarié, and Brühwiler 2006; Brühwiler and Denarié 2013; Brühwiler et al. 2015). Being possible to easily double the flexural capacity of a slab, punching shear becomes critical, especially if one thinks that it is desirable to adopt a single strengthening method to solve both flexural and punching shear strength deficiencies of a given slab. Only a few experimental studies are available concerning the punching

strength of the RC slabs strengthened with UHPFRC layers (Wuest 2007; Bastien-Masse and Brühwiler 2015; Youm and Hong 2018). A model was proposed by (Bastien-Masse and Brühwiler 2016) for determining the centred punching shear strength which is based on the failure criterion of the Critical Shear Crack Theory (CSCT) (Muttoni 2008) suitably adapted to include the effect of the UHPFRC layer. In this work, we present the outcomes of an experimental study extending the scarce existing data to include the effect of additional variables, such as the load eccentricity, shape of the concrete column and reinforcement ratio of the RC substrate and UHPFRC layer. Whenever applicable, the results are compared to the estimates provided by the existing model.

In the following, the notation RC-U refers hybrid sections with plain UHPFRC overlay over an RC substrate, while notation and RC-RU denotes the same type of section but with a reinforced UHPFRC layer. A slab containing a reinforced concrete overlay is denoted by RC-RC.

2. Failure criterion

The CSCT was originally formulated for determining the punching shear strength of RC flat slabs without transverse reinforcement (Muttoni 2008). According to the CSCT, the punching shear resistance, V_c, of the RC substrate depends on the opening of the critical shear crack, w, - assumed to be correlated to the product of the slab rotation, ψ, by the effective depth, d_{sc} - via the semi-empirical hyperbolic failure criterion set by Eq. (1). The failure criterion also contemplates the effect of the maximum aggregate size, d_g, - which accounts for the roughness of the critical shear crack -, and of the concrete strength, f_c. The control surface is determined by the product of the effective depth of the RC section, d_{sc}, by the control perimeter, b_0, defined at the distance $d_{sc}/2$ from the column face.

$$\frac{V_c}{b_0 d_{sc}\sqrt{f_c}} = \frac{3/4}{1+15\frac{\psi d_{sc}}{d_{g0}+d_g}} \tag{1}$$

The punching shear failure force is determined by the intersection of the load-rotation curve of the slab with the failure criterion (Muttoni 2008).

In the context of strengthening of existing slabs, the CSCT can be readily applied for RC-RC sections considering that if the substrate is not cracked at the time of strengthening, the maximum crack width and the critical surface are calculated using the effective depth of the overlay reinforcement, d_{sc2}, and the corresponding control perimeter, $b_{0,sc2}$ (Lapi et al. 2018a).

A composite failure criterion (CFC) that includes the contribution of the UHPFRC layer, V_U, to the punching shear resistance for RC-U and RC-RU hybrid sections was proposed by (Bastien-Masse and Brühwiler 2016), such that $V_R=V_c+V_U$, being V_R the punching shear strength of the hybrid RC-RU (or RC-U) slab. The contribution V_U depends on the concrete tensile strength, f_{ct}, which controls the development of the near interface crack (NIC) at a radius r_U, measured at the top of the slab, see Figure 1. Being the R-UHPFRC layer macro-crack free due to its improved tensile behaviour, the critical shear crack, and the subsequent punching shear failure mode, can only develop after the NIC promotes the separation between the RC substrate and the UHPFRC strengthening layer. It has been postulated by (Bastien-Masse and Brühwiler 2016) that the NIC must have the minimum dimension in the radial direction equal to the thickness of the UHPFRC layer, h_U, so that the punching shear failure mode becomes cinematically admissible. The force required to open the NIC is determined assuming a constant tensile stress distribution equal to f_{ct} at the instant of failure. In the case of centred punching around a circular column, the maximum contribution of the UHPFRC layer, V_U is then given by (2).

$$V_U = 2\pi f_{ct} h_U (r_U + h_U/2) \tag{2}$$

It has to be noted that in (2) no direct contribution of UHPFRC strength is accounted for, and no distinction is made between plain (U) or reinforced (RU) layers. However, as schematically depicted in Figure 1, the RU or U layers have a direct effect on the slab flexural stiffness, allowing the intersection between the punching force-rotation curve and the CFC failure criterion to occur at higher load levels, therefore enabling significant punching shear strength enhancement.

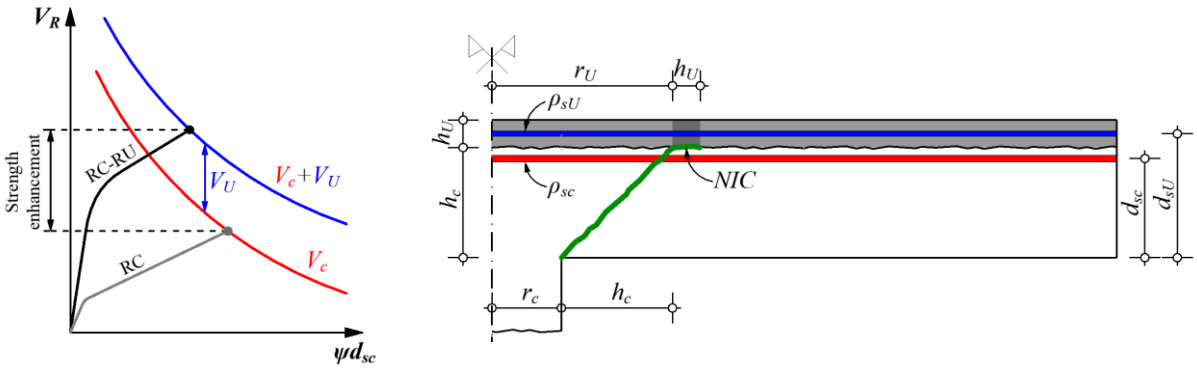

Figure 1. Determination of the punching shear strength of hybrid RC-RU (or RC-U) slabs.

3. Experimental campaign

3.1. Specimens specifications

An experimental campaign comprising tests on eight flat-slab specimens was undertaken. Five slabs were tested applying the punching force centred on a 250x250mm^2 steel plate, comprising: one reference RC slab (PRC), one RC slab with minimum flexural reinforcement strengthened with an RC layer (PC-RC) and another with an RU layer (PC-RU), one RC slab strengthened with a plain UHPFRC layer (PRC-U) and another with RU layer (PRC-RU) (see Figure 2). Of the three remaining slabs, one was tested applying the force over a 375x175mm^2 rectangular steel plate (PRC-R-RU), another over a square 250x250mm^2 concrete column segment (PE-RU1) and finally another tested with 150 mm eccentricity of the vertical force (PE-RU2)

All slabs have an octagonal shape circumscribed by a circumference with 2435 mm diameter. The PRC and PE specimens are reinforced with a square mesh #ϕ12@125 in the RC substrate, whereas PC specimens contain only #ϕ8@200. All RC substrates have a height h_c=180 mm. Both RC (h_{c2}=60 mm) and RU (h_U=40 mm) overlays are reinforced with #ϕ10@100, having and 20 and 10 mm reinforcement cover, respectively. The actual effective depths of the slabs were assessed from the cut slabs cross-sections, after the punching tests. The substrate reinforcement effective depths (d_{sc}) and respective reinforcement ratio (ρ_{sc}) are given in Table 1. The effective depth of the reinforcements in the RC and RU overlays is d_{sc2}=210 mm and d_{sU}=200 mm, respectively.

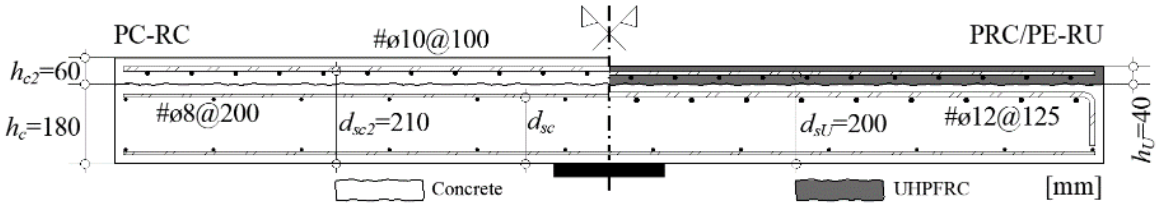

Figure 2. Specimen cross-sections.

Table 1. Effective depths and reinforcement ratios of RC substrate.

Specimens	**PRC**	**PRC-U**	**PRC-RU**	**PRC-R-RU**	**PE-RU1**	**PE-RU2**	**PC-RU**	**PC-RC**
d_{sc} **[mm]**	142	146	159	158	154	147	151	152
ρ_{sc} **[%]**	0.64	0.62	0.57	0.57	0.59	0.62	0.17	0.17

3.2. Materials

Both substrate and conventional overlay were cast with ready-mix normal strength concrete (NSC) with maximum aggregate size d_g=16 mm. The cylinder compressive strength at the age of testing ranged from

f_c=32.1 to 39.5 MPa. The corresponding split tensile strength ranged from $f_{ct,sp}$=2.9 to 3.4 MPa. For the determination of V_U according to (2), f_{ct} was determined from the compressive strength as $f_{ct}=0.3(f_c\text{-}8)^{2/3}$.

The UHPFRC was mixed in the laboratory, and consisted in a self-compacting commercial mixture, containing fibre volume ratio V_f=2% of 15 mm length (l_f) straight steel fibres with diameter d_f=0.2 mm. At 33 days, the average compressive strength on 100 mm cubes reached f_{Uc}=182 MPa and the Young modulus E_U=59 GPa. The tensile response was evaluated using direct tensile tests on dog-bone shaped specimens with cross-section of 30x40 mm^2. An average post cracking tensile strength f_{Utu}=10.2 MPa was achieved. Image analysis on polished surfaces parallel to the main fracture surface revealed that the average fibre orientation factor in the dog-bone specimens was close to 0.53, being therefore representative of a random fibre orientation in a thin UHPFRC layer.

Ordinary S500 hot-rolled ribbed steel bars were used as reinforcement.

3.3. Specimens preparation

Both overlay types were prepared in same conditions, as it would be expected in real strengthening applications. The RC substrate surfaces were hydro-jetted (see Figure 3(a)) removing nearly 10 mm of concrete and exposing the coarse aggregate. An average roughness depth R_t=6.3 mm was achieved, being assessed using the sand patch test method (SPM) (ASTM 2001).

(a) (b)

Figure 3. Specimens preparation: (a) hydro-jetting; and (b) UHPFRC overlay casting.

Prior to casting (see Figure 3(b)), the interface was saturated. Before the punching tests, pull-off tests were performed to assess the interface tensile bond strength between the substrate and overlayers. About 75% of the cores from the RC overlay failed on the interface, whereas, 100% of the RU failed at the substrate.

3.4. Punching test setup, instrumentation and procedure

The punching tests were conducted under displacement control of the hydraulic actuator exerting the force at the central part of the specimens (150 mm eccentric in the case of specimen PE-RU2) at a rate of 0.01 mm/sec. Eight reaction plates (120x120x25 mm^3) were distributed along the line of contra-flexure defined by the radius r_q=1082 mm. The load was applied from bottom to top by a 1500 kN capacity hydraulic actuator equipped by a load cell, placed upside down on the reaction slab of the laboratory. The reaction plates were anchored to the reaction slab through ϕ32 mm DYWIDAG bars.

The vertical displacements were measured on the top surface of the slabs using 11 LVDTs fixed to an independent steel frame along two orthogonal alignments following the orthogonal reinforcement directions.

The punching shear failure was characterized by a sudden drop of the load soon after the peak being reached. After that, the post-peak load for the majority of the specimens barely increased and no more than 10 minutes later the tests were stopped.

After the punching tests, the top cracks were marked and then the slabs were cut along the central alignments. The actual reinforcement depths and the critical shear cracks angles were measured.

4. Results and discussion

Hereafter, the experimental results are presented either by absolute or normalized load-rotation/central displacement curves. The corresponding punching shear force and rotations are presented in Table 2. The rotations, ψ, are calculated as $\psi = \delta/(r_q - r'_c)$, where δ is the relative vertical displacement of the centre point of the slab with respect to the 8 support plates, r_q is the radius of the circumference passing by the support plates and r'_c is the radius of a circumference with the same perimeter as that of the loading area. In the case of the rectangular loading area this provides an average rotation in the two orthogonal directions. Whenever applicable, the corresponding failure criterion is also depicted. In this regard, it is recalled that the CFC failure criterion does not normalize similarly to that of the CSCT due to the variables f_{ct} and h_U according to (2).

Table 2. Experimental results.

Specimens	**PRC**	**PRC-U**	**PRC-RU**	**PRC-R-RU**	**PE-RU1**	**PE-RU2**	**PC-RU**	**PC-RC**
V_R **[kN]**	431	682	1024	952	940	686	929	764
ψ **[‰]**	25.8	19.1	12.4	9.2	8.6	-	14.8	25.1

The UHPFRC contribution is herein evaluated by comparing the reference slab PRC with the strengthened slabs with plain and the reinforced UHPFRC, PRC-U and PRC-RU, respectively. The respective normalized load-rotation curves are shown in Figure 4(a). The significant stiffness increase provided by the strengthening layers is evident, even in the case of the plain UHPFRC layer. The punching shear strength of the PRC-U and PRC-RU slabs increased 1.58 and 2.38 times, respectively, with respect to the reference PRC. The failure loads are reasonably well predicted using the CSCT and the CFC, with the ratios $V_{R,exp}/V_{R,calc}$=1.06, 0.99 and 1.09, respectively for PRC, PRC-U and PRC-RU. Figure 4(a) also shows the results of the slab with rectangular loaded area, PRC-R-RU. Despite the perimeter of the load area being the same, the punching shear strength was 91% of that of slab with the square load area (PRC-RU).

The comparison between the reinforcement ratio of the substrate reveal an unanticipated high initial stiffness of that slab with the lower reinforcement ratio in the substrate ρ_{sc}=0.17% (PC-RU) (see Figure 4(b)). The punching shear strength was not greatly affected by the reduced reinforcement ratio, as it can be concluded comparing the curves of the PC-RU and PRC-RU slabs (the latter with ρ_{sc}=0.57%). This fact confirms the assumptions behind the calculation of the punching shear strength using the CFC: being the flexural stiffness essentially controlled by the strengthening layer, and not so much by the reinforcement in the existing RC substrate, the intersection with the CFC occurs for similar load levels.

Overall, the results of the hybrid slabs subjected to centered punching confirm the adequacy of the CFC proposed by Bastien-Masse and Brühwiler (2016) and of the approach based on the CSCT.

The contribution of the RU relatively to RC strengthening layers is compared in Figure 5(a) by means of absolute load-rotation curves of the slabs PC-RC and PC-RU. The comparison with the CSCT failure criterion shows that the rotation at failure of PC-RC slab exceed that predicted by the CSCT. It is noted stiffer response of the PC-RU specimen and the 1.22 times higher failure load, despite the total depth of slab being 20 mm lower compared to the slab PC-RC. However, the ultimate rotation at failure decreased about 40% compared to the specimens PRC and PC-RC.

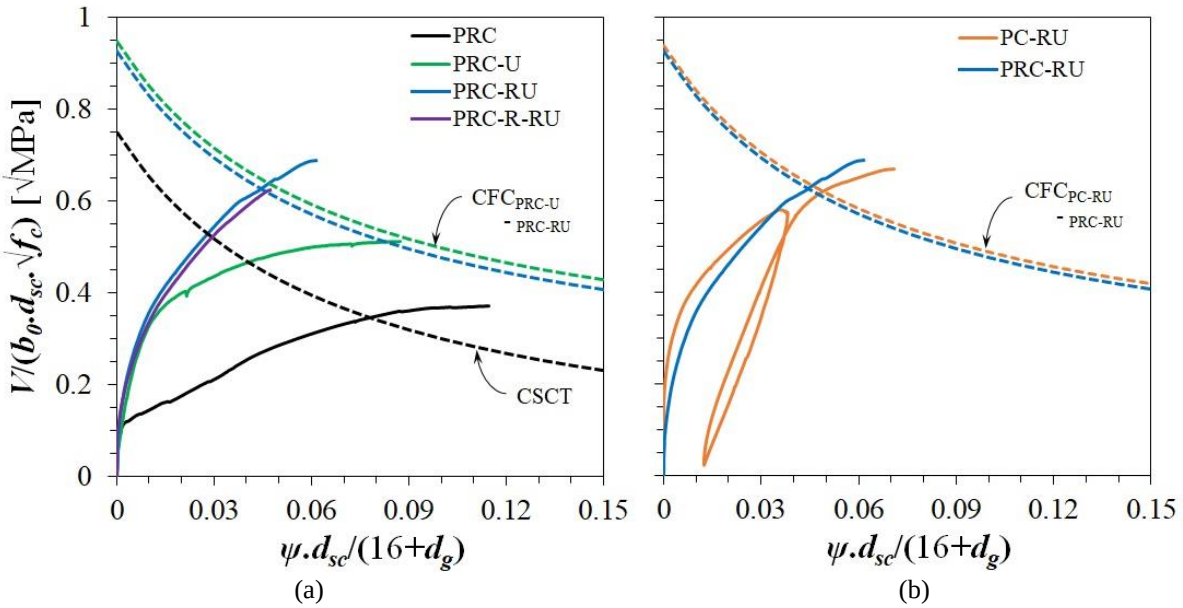

Figure 4. Normalized experimental load-rotation curves: (a) effect of UHPFRC layer contribution and shape of the loading area; and (b) effect of the reinforcement ratio in the substrate.

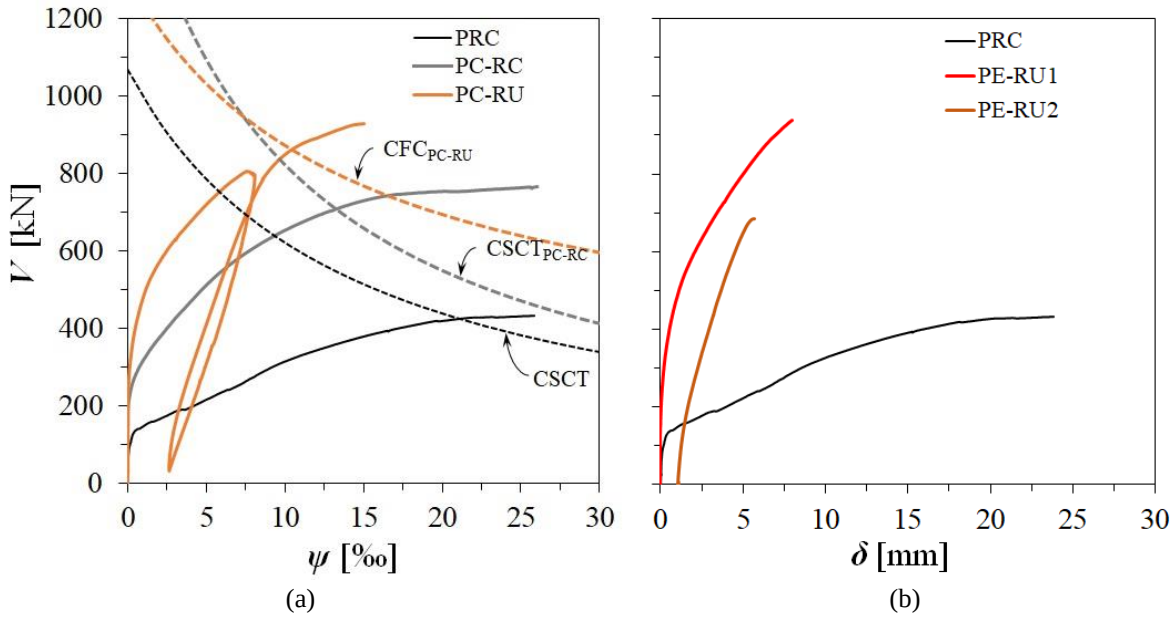

Figure 5. Experimental curves: (a) comparison between RC and RU layers; and (b) effect of the force eccentricity.

The crack patterns of the PC-RC and PC-RU slabs that could be detectable by the naked eye are compared in Figure 6. The crack pattern in the PC-RC slab is clearly more developed. However, the PC-RU slab exhibits a fine micro-crack pattern (not represented), with cracks spaced around 10 to 20 mm, and which can only be detected after spraying the surface with alcohol. This type of crack pattern was observed in all the specimens with reinforced UHPFRC layer. In the PRC-U specimen, without rebars in the strengthening layer, these fine micro-crack pattern could not be detected even after spraying the surface with alcohol.

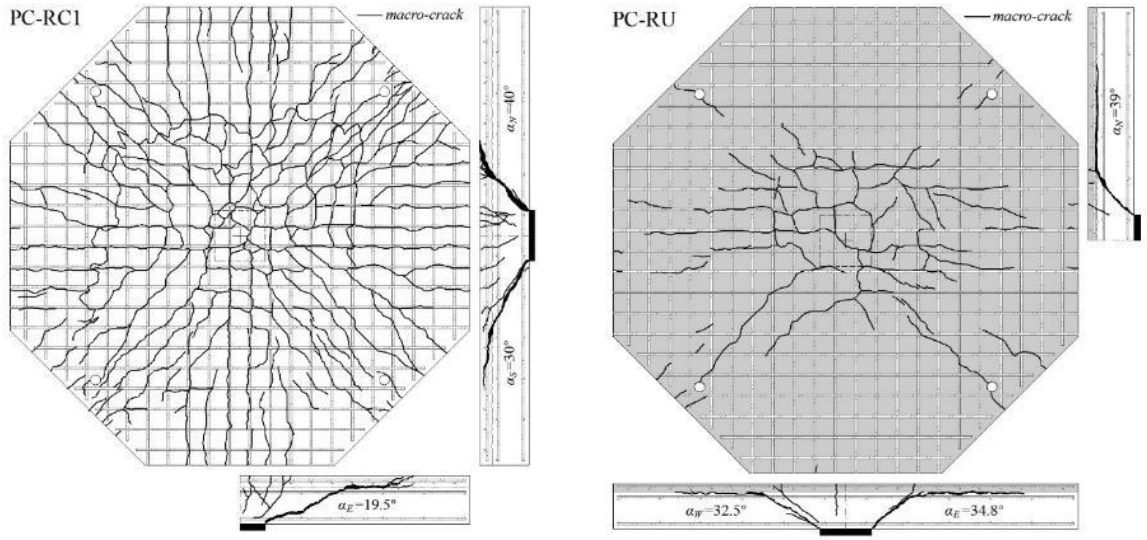

(a) (b)

Figure 6. Cracking pattern of PC slabs: (a) PC-RC; and (b) PC-RU (only cracks visible to the naked eye are marked).

The saw cuts are also presented in Figure 6. It can be seen that while the critical shear crack of the PC-RC slab crosses the slab full depth (Figure 6(a)), in PC-RU the inclined shear crack does not cross through the UHPFRC layer and propagates horizontally just below the interface between the two materials (Figure 6(b)). This was observed in all the slabs strengthened with a UHPFRC layer.

Finally, the effect of the 150 mm force eccentricity effect introduced in the PE-RU2 is analysed. The force versus central vertical displacement of the slabs where the force was applied on a 250x250 mm^2 concrete column segment monolithic with the slab are shown in Figure 5(b). In the case of the slab with the 150 mm eccentricity (PE-RU2), the initial part of the load-deflection curve is missing and only the reloading branch is available. The punching shear strength is 27% lower than that of the concentrically loaded PE-RU1.

5. Conclusion

An experimental campaign consisting of 6 RC flat slabs strengthened with UHPFRC layer tested under punching shear was undertaken, complemented with one reference specimen and one specimen strengthened with an RC layer. Several variables that affect the contribution of the UHPFRC were assessed, namely the reinforcement ratio in the existing slab, the reinforcement in the strengthening layer, the shape of the column and the force eccentricity.

The results have shown the significant contribution of the UHPFRC layers to the punching shear capacity. The punching shear strength increased 1.58 and 2.38 times with respect to the reference PRC specimen by adding an unreinforced (specimen PRC-U) or reinforced (PRC-RU) 40 mm thick UHPFRC layer, respectively.

Concerning the comparison between slabs containing just the minimum flexural reinforcement, the strengthening efficiency of adding a conventional RC layer was compared to that of an R-UHPFR layer, the latter allowing a substantial increase in the stiffness and punching shear strength, at the cost of the reduction of the deformation capacity at failure.

The effect of the shape of the loaded area revealed to be moderate. Two loading area shapes were tested, with approximately the same perimeter, one being square and the other rectangular with a=2b. The punching shear strength of the latter was 9% smaller. As for the effect of the load eccentricity, e, the hybrid slab tested with e=150 mm (=0.6 times the column side), failed at about 75% of the force of the slab tested under concentric loading.

The slabs with reinforced UHPFRC layers exhibited a fine microcrack pattern, with the micro-cracks spaced every 10 to 20 mm, only visible after spraying the surface with alcohol. This fine micro-crack pattern was not present in the slab strengthened with the plain UHPFRC layer. The saw cuts revealed that the critical shear crack does not cross the UHPFRC layer and propagates horizontally just below the interface between the two materials.

Finally, the application of the composite failure criterion based on the CSCT has shown to predict quite well the punching shear strength of the concentrically loaded slabs and with square loading area.

Acknowledgements

The authors acknowledge the financial support by: Base (UIDB/04708/2020) and Programmatic (UIDP/04708/2020) funding of CONSTRUCT financed by national funds through the FCT/MCTES (PIDDAC); project HiperSlab (PTDC/ECI-EST/30511/2017) financed by national funds through FCT/MCTES (PIDDAC).

The support by Laboratório de Engenharia de Moçambique (LEM) and Fundação Calouste Gulbenkian through the PhD grant nº144945 attributed to the first author are gratefully acknowledged. Collaboration of the companies Gabriel Couto, LimpaCanal and RasgAbre is gratefully acknowledged.

References

ASTM. 2001. "Standard Test Method for Measuring Pavement Macrotexture Depth Using a Volumetric Technique: E 965." ASTM.

Bastien-Masse, Malena, and Eugen Brühwiler. 2015. "Experimental Investigation on Punching Resistance of R-UHPFRC–RC Composite Slabs." *Materials and Structures* 49: 1573–90. https://doi.org/10.1617/s11527-015-0596-4.

———. 2016. "Composite Model for Predicting the Punching Resistance of R-UHPFRC–RC Composite Slabs." *Engineering Structures* 117: 603–16. https://doi.org/10.1016/j.engstruct.2016.03.017.

Brühwiler, Eugen, Malena Bastien-Masse, Hartmut Mühlberg, Bernard Houriet, Blaise Fleury, Stéphane Cuennet, Philippe Schär, Frédéric Boudry, and Marco Maurer. 2015. "Strengthening the Chillon Viaducts Deck Slabs with Reinforced UHPFRC." In *IABSE Conference – Structural Engineering: Providing Solutions to Global Challenges*. Geneva.

Brühwiler, Eugen, and Emmanuel Denarié. 2013. "Rehabilitation and Strengthening of Concrete Structures Using Ultra-High Performance Fibre Reinforced Concrete." *Structural Engineering International* 23 (4): 450–57. https://doi.org/10.2749/101686613X13627347100437.

Fernandes, Hugo Daniel Pereira. 2019. "Strengthening of Flat Slabs with Reinforced Concrete Overlay – Analysis and Development of the Solution." Universidade Nova de Lisboa.

Gardner, N. J., Jungsuck Huh, and Lan Chung. 2002. "Lessons from the Sampoong Department Store Collapse." *Cement and Concrete Composites* 24 (6): 523–29. https://doi.org/10.1016/S0958-9465(01)00068-3.

Habel, Katrin, Emmanuel Denarié, and Eugen Brühwiler. 2006. "Structural Response of Elements Combining and Reinforced Concrete." *Journal of Structural Engineering* 132 (November): 1793–1800. https://doi.org/10.1061/?ASCE?0733-9445?2006?132:11?1793?

King, Suzanne, and Norbert J. Delatte. 2004. "Collapse of 2000 Commonwealth Avenue: Punching Shear Case Study." *Journal of Performance of Constructed Facilities* 18 (1): 54–61. https://doi.org/10.1061/(asce)0887-3828(2004)18:1(54).

Koppitz, Robert, Albin Kenel, and Thomas Keller. 2013. "Punching Shear of RC Flat Slabs – Review of Analytical Models for New and Strengthening of Existing Slabs." *Engineering Structures* 52: 123–30. https://doi.org/10.1016/J.ENGSTRUCT.2013.02.014.

Lapi, Massimo, Hugo Fernandes, Maurizio Orlando, António Ramos, and Válter Lúcio. 2018a. "Performance Assessment of Flat Slabs Strengthened with a Bonded Reinforced-Concrete Overlay." *Magazine of Concrete Research* 70 (9): 433–51. https://doi.org/10.1680/jmacr.17.00037.

Lapi, Massimo, Hugo Fernandes, Maurizio Orlando, António Pinho Ramos, and Válter Lúcio. 2018b.

"Performance Assessment of Flat Slabs Strengthened with a Bonded Reinforced Concrete Overlay." *Magazine of Concrete Research* 70 (9): 433–51. https://doi.org/doi.org/10.1680/jmacr.17.00037.

Lapi, Massimo, António Pinho Ramos, and Maurizio Orlando. 2019. "Flat Slab Strengthening Techniques against Punching-Shear." *Engineering Structures* 180: 160–80. https://doi.org/10.1016/j.engstruct.2018.11.033.

Lew, H. S., N. J. Carino, S.G. Fattal, and M. E. Batts. 1982. "Investigation of Construction Failure of Harbour Cay Condominium in Cocoa." Washington, DC. https://doi.org/10.6028/NBS.BSS.145.

Muttoni, Aurelio. 2008. "Punching Shear Strength of Reinforced Concrete Slabs without Transverse Reinforcement." *ACI Structural Journal* 105 (4): 440–50.

Wood, Jonathan G. M. 2003. "Pipers Row Car Park Wolverhampton: Quantitative Study of the Causes of the Partial Collapse on 20th March 1997." *Health and Safety Executive*. The United Kingdom.

Wuest, John. 2007. "Comportement Structural Des Bétons de Fibres Ultra Performants En Traction Dans Des Éléments Composés." École Polytchnique Fédérale de Lausanne.

Youm, H S, and S G Hong. 2018. "Evaluation for Punching Shear Strength of Slab-Column Connections with Ultra High Performance Fiber-Reinforced Concrete Overlay." *International Journal of Structural and Construction Engineering* 12 (1): 56–61.